

Magnetostatic interactions between magnetic nanotubes

J. Escrig, S. Allende, D. Altbir and M. Bahiana

Departamento de Física, Universidad de Santiago de Chile,

USACH, Av. Ecuador 3493, Santiago, Chile and

Instituto de Física, Universidade Federal do Rio de Janeiro, CP 68528, 21941-972 Rio de Janeiro, Brazil

The investigation of interactions between magnetic nanotubes is complex and often involves substantial simplifications. In this letter an analytical expression for the magnetostatic interaction, taking into account the geometry of the tubes, has been obtained. This expression allows for the definition of a critical vertical separation for relative magnetization between nanotubes and can be used for tailoring barcode-type nanostructures with prospective applications such as biological separation and transport.

Since the discovery of carbon nanotubes by Iijima in 1991,¹ intense attention has been paid to tubular nanostructures. Because of their geometry, nanotubes offer prospective applications in catalysis,^{2,3} sensors,⁴ and biological separation and transport.^{3,5-7} In particular, magnetic nanotubes are the focus of growing interest due to the existence of techniques that lead to the production of highly ordered arrays.⁸⁻¹⁰ These particles offer an additional degree of freedom as compared to nanowires; not only can the length, L , and external radius, R , be varied, but also the internal radius, a . In this way, nanotubes may be suitable for applications in biotechnology, where magnetic nanostructures with low density, which can float in solutions, become much more useful for in vivo applications.¹¹ These tiny magnetic tubes could provide an unconventional solution for several research problems, and a useful vehicle for imaging and drug delivery applications.^{7,12}

In such systems changes in thickness are expected to strongly affect the mechanism of magnetization reversal¹³ and, thereby, the overall magnetic behavior. Also interactions play a fundamental role, modifying the magnetic behavior of the particles. Clearly, for the development of magnetic devices based on those arrays, knowledge of the magnetostatic interaction between the tubes is of fundamental importance. But as usual the effects of interparticle interactions are complicated by the fact that the dipolar field felt by each element depends upon the magnetization state of all the elements in the array. In a previous work by Lee *et. al.*,¹⁴ multisegmented metallic nanotubes with a bimetallic stacking configuration along the nanotube axes were prepared and investigated. These particles exhibit different magnetic behaviors, which encourage a study about the magnetostatic interactions between the stacking. Due to the very narrow hysteresis loops that are obtained, the influence of the interactions is not easily identifiable from magnetization curves, and then a theoretical study can shine light on this problem.

The purpose of this letter is to develop an analytical model for the full long-range magnetostatic interaction between two nanotubes exploring the possibility of varying the magnetic coupling as a function of the tubes position. The geometry of the tubes is characterized by their external and internal radii, R and a , respectively, and

length L . It is convenient to define the ratio $\beta \equiv a/R$, so that $\beta = 0$ represents a solid cylinder (wire) and β close to 1 corresponds to a tube with very thin walls. The separation between the tubes is written in terms of the inter-axial distance, d , and the vertical separation, s , as depicted in Fig. 1. Our model goes beyond the dipole-dipole approximation and lead us to obtain an analytical expression for the interaction in which the lengths and radii of the tubes are taken into account. We focus on the stability of parallel and antiparallel magnetization alignment in pairs of interacting tubes, as a function of the distance between them, in order to gain insight on the understanding of the role of interactions on barcode-type nanotubes.^{14,15}

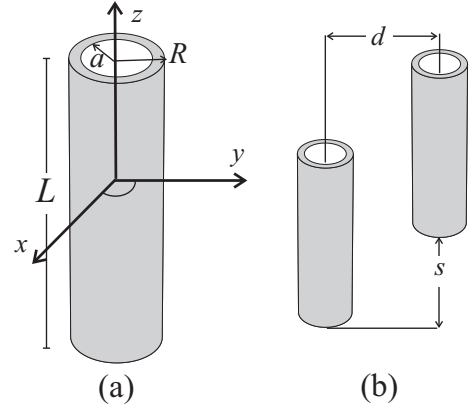


FIG. 1. (a) Geometric parameters used for the individual tube description. (b) Relative position of interacting tubes: d is the inter-axial distance and s the vertical separation.

We adopt a simplified description of the system, in which the discrete distribution of magnetic moments is replaced with a continuous one characterized by a slowly varying magnetization $\mathbf{M}(\mathbf{r})$. The total magnetization can be written as $\mathbf{M}(\mathbf{r}) = \mathbf{M}_1(\mathbf{r}) + \mathbf{M}_2(\mathbf{r})$, where $\mathbf{M}_1(\mathbf{r})$ and $\mathbf{M}_2(\mathbf{r})$ are the magnetization of tubes 1 and 2, respectively. In this case, the magnetostatic potential $U(\mathbf{r})$ splits up into two components, $U_1(\mathbf{r})$ and $U_2(\mathbf{r})$, associated with the magnetization of each individual tube. Then, the magnetostatic energy of two interacting magnetic tubes may be written in terms of their magnetiza-

tions and the fields generated by each one. The general expression, after using the reciprocity theorem, is $E_d = E_{\text{self}}^1 + E_{\text{self}}^2 + E_{\text{int}}$. The $E_{\text{self}}^i = \frac{\mu_0}{2} \int \mathbf{M}_i(\mathbf{r}) \cdot \nabla U_i(\mathbf{r}) dV_i$ terms correspond to the self-energy of the i -th tube, and $E_{\text{int}} = \mu_0 \int \mathbf{M}_2(\mathbf{r}) \cdot \nabla U_1(\mathbf{r}) dV_2$ is the interaction energy between tubes, which is the focus of this letter.

In order to proceed, we first need to calculate the magnetostatic potential $U(\mathbf{r})$ of a single tube. However, it is necessary to specify the functional form of the magnetization for each nanotube. Due to their geometry and in order to reduce the stray field, tubes present what is called a flower configuration.¹⁶ In this case, the magnetization is mostly homogeneous, and spreads outwards near the ends. This non-homogeneity produces a decrease of the interaction energy felt by one tube due to the other. For $L \gg R$ this decrease is small and can be neglected to simplify the calculations. Thus, we consider tubes with an axial magnetization defined by $\mathbf{M}_i(\mathbf{r}) = M_0 \sigma_i \hat{\mathbf{z}}$, where M_0 is the saturation magnetization of each nanotube, $\hat{\mathbf{z}}$ is the unit vector parallel to the axis of the nanotube and σ_i takes the values ± 1 , allowing the magnetization of tube i to point up ($\sigma_i = +1$) or down ($\sigma_i = -1$) along $\hat{\mathbf{z}}$. The magnetostatic potential produced by the tube 1 with magnetization $\mathbf{M}_1(\mathbf{r})$ is given by volume and surface contributions and can be written as

$$U_1(\mathbf{r}) = \frac{1}{4\pi} \left[- \int_{V_1} \frac{\nabla \cdot \mathbf{M}_1(\mathbf{r}')}{|\mathbf{r} - \mathbf{r}'|} dV' + \int_{S_1} \frac{\hat{\mathbf{n}}' \cdot \mathbf{M}_1(\mathbf{r}')}{|\mathbf{r} - \mathbf{r}'|} dS' \right]. \quad (1)$$

Note that the first term on the right-hand side of Eq. (1) vanishes because the magnetization field is constant. Furthermore, the surface integral in Eq. (1) has contributions only from the upper and lower ends of the tube, located at $z = L/2$ and $z = -L/2$, respectively. Due to the symmetry of the problem, we have calculated the integral in (1) using a kernel in cylindrical coordinates.¹⁷ After some manipulation, the integral expression for the scalar potential can be written as

$$U_1(r, z) = \sigma_1 \frac{M_0}{2} \int_0^\infty \frac{dk}{k} J_0(kr) \left[R J_1(kR) - a J_1(ka) \right] \left(e^{-k|\frac{L}{2}-z|} - e^{-k|-\frac{L}{2}-z|} \right), \quad (2)$$

where $J_n(x)$ is the n -th order Bessel function of first kind. Figure 2 shows the surface plot of U_1 for a thin-walled tube ($\beta = 0.8$) and a wire ($\beta = 0$). From this figure it is clear that one should expect distinct behaviors from these two nanoelements in the region near the ends.

Now it is possible to calculate the magnetostatic interaction energy between two identical nanotubes using the magnetostatic field experienced by one of the tubes due to the other. The final result reads

$$\tilde{E}_{\text{int}} = - \frac{\sigma_1 \sigma_2}{(1 - \beta^2)} \int_0^\infty \frac{dq}{q^2} J_0\left(\frac{d}{L} q\right) e^{-q(1 + \frac{s}{L})} \left[J_1\left(\frac{R}{L} q\right) - \beta J_1\left(\frac{R}{L} q \beta\right) \right]^2 \begin{cases} (1 - e^q)^2 & s \geq L \\ (1 - 2e^q + e^{2q \frac{s}{L}}) & s \leq L \end{cases} \quad (3)$$

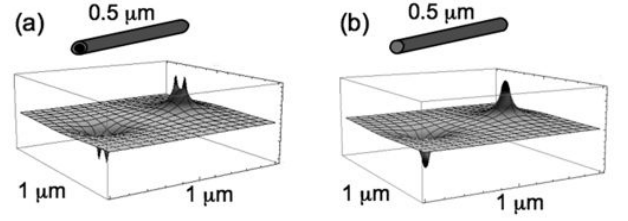


FIG. 2. Magnetostatic potential $U(\mathbf{r})$ according to equation (2) produced by a tube with $L = 500$ nm, $R = 50$ nm, and (a) $\beta = 0.8$ (thin-walled tube) and (b) $\beta = 0$ (wire). The color scale is chosen such that higher absolute values of U are represented by darker shades.

Here \tilde{E}_{int} is the interaction energy in units of $\mu_0 M_0^2 V$, i.e. $\tilde{E}_{\text{int}} \equiv E_{\text{int}} / \mu_0 M_0^2 V$, where $V = \pi R^2 L (1 - \beta^2)$ is the volume of a tube. Equation (3) has been previously obtained for nanowires ($\beta = 0$) for $s = 0$ nm.^{18,19} The general expression for the interaction energy between tubes with axial magnetization, given by equation (3), can only be solved numerically. However, tubes that motivated this work⁸⁻¹⁰ satisfy $R/L = \alpha \ll 1$, in which case one can use that $J_1(\alpha x) \approx \alpha x/2$. With this approximation, Eq. (3) can be written in a very simple form as

$$\tilde{E}_{\text{int}} = - \frac{\sigma_1 \sigma_2 R^2 (1 - \beta^2)}{4Ld} \left[\frac{1}{\sqrt{1 + (\frac{L-s}{d})^2}} - \frac{2}{\sqrt{1 + (\frac{s}{d})^2}} + \frac{1}{\sqrt{1 + (\frac{L+s}{d})^2}} \right]. \quad (4)$$

The simplicity of Eq. (4) makes it an excellent tool for the understanding of interactions between those nanoelements. Figure 3 illustrates the interaction energy, obtained from Eq. (4), between two identical nanotubes with parallel axial magnetization as a function of $2R/d$. When the two tubes are in contact, $2R/d = 1$; when they are infinitely separated, $2R/d = 0$. Differences between this expansion and the full expression in Eq. (3) are less than 3% for any L/R . As an illustration, when we consider two Ni nanotubes ($\beta = 0.8$) with $L = 500$ nm, $R = 50$ nm, $s = 100$ nm and $d = 100$ nm, we obtain $E_{\text{int}} = 13.15$ eV from Eq. (3), and $E_{\text{int}} = 13.75$ eV from Eq. (4).

It is interesting to analyze the behavior of the interaction energy given by Eq. (4) as the inter-axis distance, d , is kept fixed and the vertical separation, s , is varied. We define the critical separation s_0 such that $\tilde{E}_{\text{int}}(L, d, s_0) = 0$. For tubes with $L = 500$ nm and $d = 100$ nm, $s_0 = 317$ nm, independently of other parameters, as depicted in Fig. (4). Since lateral positions (small s) favor antiparallel magnetization alignment, the interaction energy is positive for $s \leq s_0 = 317$ nm. For $s > s_0 = 317$ nm the interaction between tubes with parallel magnetization is attractive, the strongest attraction appearing for $s \approx 500$ nm.

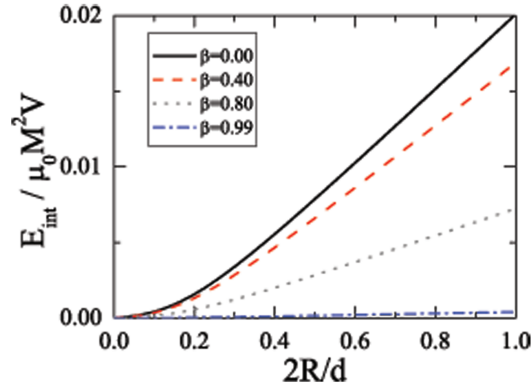


FIG. 3. (Color online) Interaction energy between two identical nanotubes, as given by Eq. (4). The tubes have $L = 500$ nm, $R = 50$ nm, different values of β and parallel magnetization defined by $\sigma_1 = \sigma_2$. The vertical position kept fixed, $s = 0$ nm, and the inter-axis distance d is varied as a function of $2R/d$.

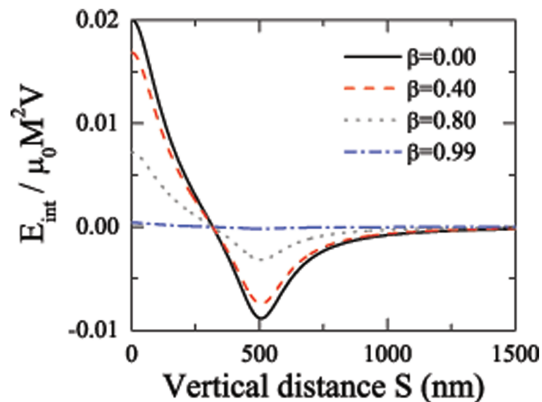


FIG. 4. (Color online) Interaction energy of two identical nanotubes, as given by Eq. (4). The tubes have $L = 500$ nm, $R = 50$ nm, different values of β and parallel magnetization defined by $\sigma_1 = \sigma_2$. The inter-axis distance kept fixed, $d = 100$ nm, and the vertical separation s is varied.

The dependence of s_0 on L for different values of d can

be seen in Fig. (5) For $L \gtrsim 2.5 \mu\text{m}$, which corresponds to values usually found in nanotubes, we observe a linear dependence of the form $s_0 = 0.62L$, almost independent of d .

In conclusion, by expanding the general expression for the magnetostatic interaction energy between tubes, and keeping the first-order term we have obtained an expression that can be easily used to calculate the magnetostatic interaction between tubes. In particular, we have

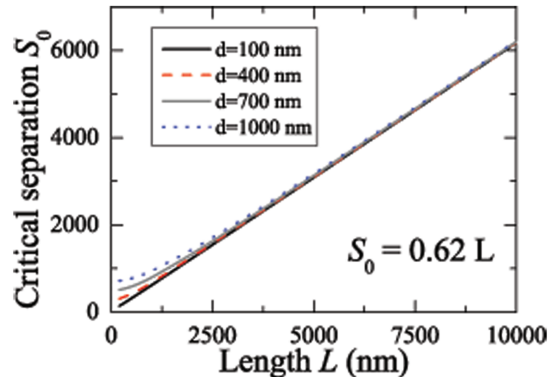


FIG. 5. (Color online) Dependence of the critical vertical separation s_0 on d and L for two identical tubes with arbitrary values of β and R . For $s < s_0$ antiparallel alignment of the magnetization is favored.

investigated the relative position of the tubes for which the ferromagnetic and antiferromagnetic configurations are of lowest energy. For the tubes usually found in the literature, $L \gtrsim 2.5 \mu\text{m}$, we observe a linear dependence of the critical vertical distance of the form $s_0 = 0.62L$. Our results are intended to provide guidelines for the production of barcode-type nanostructures with prospective applications such as biological separation and transport.

This work has been partially supported by FONDECYT (N° 11070010 and N° 1080300), Millenium Science Nucleus *Basic and Applied Magnetism* P06-022F, Departamento de Investigaciones Científicas y Tecnológicas, USACH, and AFOSR (award N° FA9550-07-1-0040) in Chile, and Instituto do Milênio de Nanotecnologia, MCT/CNPq, FAPERJ, and PROSUL/CNPq in Brazil. CONICYT Ph.D. program and Graduate Direction of Universidad de Santiago de Chile are also acknowledged.

¹ S. Iijima, *Nature* **354**, 56-58 (1991).

² M. S. Sander, M. J. Cote, W. Gu, B. M. Kile, and C. P. Tripp, *Adv. Mater.* **16**, 2052-2057 (2004).

³ D. T. Mitchell, S. B. Lee, L. Trofin, N. Li, T. K. Nevanen, H. Soderlund, and C. Martin, *J. Am. Chem. Soc.* **124**, 11864-11856 (2002).

⁴ A. Kros, R. J. M. Nolte, and N. A. J. M. Sommerdijk, *Adv. Mater.* **14** 1779-1782 (2002).

⁵ S. B. Lee, D. T. Mitchell, L. Trofin, T. K. Nevanen, H. Soderlund, and C. R. Martin, *Science* **296**, 2198-2200 (2002).

⁶ P. Kohli, C. C. Harrel, Z. Cao, R. Gasparac, W. Tan, and

- C. R. Martin, *Science* **305**, 984-986 (2004).
- ⁷ S. J. Son, J. Reichel, B. He, M. Schuchman, and S. B. Lee, *J. Am. Chem. Soc.* **127**, 7316-7317 (2005).
- ⁸ M. Daub, M. Knez, U. Gosele, H. Jeske, and K. Nielsch, *J. Appl. Phys.* **101**, 09J111 (2007).
- ⁹ J. Bachmann, J. Jing, M. Knez, S. Barth, H. Shen, S. Mathur, U. Gosele, and K. Nielsch, *J. Am. Chem. Soc.* **129**, 9554-9555 (2007).
- ¹⁰ J. Escrig, J. Bachmann, J. Jing, M. Daub, D. Altbir, and K. Nielsch, *Phys. Rev. B* **77**, 214421 (2008).
- ¹¹ M. Eisenstein, *Nature Methods* **2**, 484-484 (2005).
- ¹² J. Xie, L. Chen, V. K. Varadan, J. Yancey, and M. Srivatsan, *Nanotechnology* **19**, 105101 (2008).
- ¹³ P. Landeros, S. Allende, J. Escrig, E. Salcedo, D. Altbir, and E. E. Vogel, *Appl. Phys. Lett.* **90**, 102501 (2007).
- ¹⁴ W. Lee, R. Scholz, K. Nielsch, and U. Gosele, *Angew. Chem. Int. Ed.* **44**, 6050-6054 (2005).
- ¹⁵ S. R. Nicewarner-Peña, R. G. Freeman, B. D. Reiss, L. He, D. J. Peña, I. D. Walton, R. Cromer, C. D. Keating, and M. J. Natan, *Science* **294**, 137-141 (2001).
- ¹⁶ Riccardo Hertel, and Helmut Kronmüller, *J. Magn. Magn. Mater.* **238**, 185-199 (2002).
- ¹⁷ J. D. Jackson, *Classical Electrodynamics*, 2nd ed. (Wiley, New York, 1975).
- ¹⁸ M. Beleggia, S. Tandon, Y. Zhu, and M. De Graef, *J. Magn. Magn. Mater.* **278**, 270-284 (2004).
- ¹⁹ D. Laroze, J. Escrig, P. Landeros, D. Altbir, M. Vazquez, and P. Vargas, *Nanotechnology* **18**, 415708 (2007).